British Journal of Pharmacology (2008) 154, 246–255
 0007–1188/08 $30.00
www.brjpharmacol.org

RESEARCH PAPER

Rifampin and digoxin induction of MDR1 expression and function in human intestinal (T84) epithelial cells

IS Haslam[1], K Jones[2], T Coleman[2] and NL Simmons[1]

[1]*Epithelial Research Group, Institute for Cell and Molecular Biosciences, University of Newcastle Upon Tyne, Medical School, Newcastle Upon Tyne, UK and* [2]*AstraZeneca, Discovery DMPK, Cheshire, UK*

Background and purpose: Oral drug bioavailability is limited by intestinal expression of P-glycoprotein (MDR1, Pgp, ABCB1) whose capacity is regulated via nuclear receptors e.g. the pregnane X receptor (PXR, SXR, NR1I2). In order to study dynamic regulation of MDR1 transport capacity we have identified the T84 epithelial cell-line as a model for human intestine co-expressing MDR1 with PXR. The ability of rifampin, a known PXR agonist and digoxin, a model MDR1 substrate, to regulate MDR1 expression and transport activity has been tested, in these T84 cells.
Experimental approach: Transport was assayed by bi-directional [^{3}H]-digoxin transepithelial fluxes across epithelial layers of T84 cells seeded onto permeable filter supports following pre-exposure to rifampin and digoxin. Quantitative real-time PCR, Western blotting and immunocytochemistry were used to correlate induction of MDR1 transcript and protein levels with transport activity.
Key results: Rifampin exposure (10 μM, 72 hours) increased MDR1 transcript levels (3.4 fold), MDR1 total protein levels (4.4 fold), apical MDR1 protein (2.7 fold) and functional activity of MDR1 (1.2 fold). Pre-incubation with digoxin (1 μM, 72 hours) potently induced MDR1 transcript levels (92 fold), total protein (7 fold), apical MDR1 protein (4.7 fold) and functional activity (1.75 fold). Whereas PXR expression was increased by rifampin incubation (2 fold), digoxin reduced PXR expression (0.3 fold).
Conclusions and implications: Chronic digoxin pre-treatment markedly upregulates MDR1 expression and secretory capacity of T84 epithelia. Digoxin-induced changes in MDR1 levels are distinct from PXR-mediated changes resulting from rifampin exposure.
British Journal of Pharmacology (2008) **154,** 246–255; doi:10.1038/bjp.2008.69; published online 10 March 2008

Keywords: digoxin; rifampin; T84 cells; P-glycoprotein; pregnane X receptor; constitutive androstane receptor; induction

Abbreviations: ABC, ATP-binding cassette; CAR, constitutive androstane receptor; MDR1, multidrug resistance 1; Pgp, P-glycoprotein; PXR, pregnane X receptor

Introduction

The oral availability, disposition and pharmacokinetic profile of a diverse range of drug molecules are controlled by the operation of members of the ATP-binding cassette (ABC) family, including P-glycoprotein (multidrug resistance 1 (MDR1), P-glycoprotein, ABCB1) (Schinkel *et al*., 1997), multidrug resistance-related protein 2 (cMOAT, ABCC2) (Vlaming *et al*., 2006) and breast cancer resistance protein (MXR, ABCG2) (Allen *et al*., 2002; Jonker *et al*., 2002). At the intestinal brush-border, ABC-mediated secretory efflux of drug compounds to the intestinal lumen (for example, digoxin via MDR1) reduces the effective absorptive permeability, thereby reducing peak circulatory plasma concentrations and reducing therapeutic efficacy (Hunter *et al*., 1991, 1993; Cavet *et al*., 1996; Lowes and Simmons, 2002; Drescher *et al*., 2003). The expression of MDR1 and other efflux transport proteins is not static, but is regulated dynamically via transcriptional control by certain nuclear receptors acting as 'xenosensors'. Examples include the pregnane X receptor (pregnane X receptor (PXR), SXR, NR1I2) and the constitutive androstane receptor (CAR, NR1I3) (Burk *et al*., 2005; Cerveny *et al*., 2007) whose overlapping specificities form a 'xenosensor' network of regulating effectors, which include both metabolism and transport.

The specificity of nuclear receptors, including PXR, have been characterized by gene-based reporter assays (Luo *et al*., 2002, 2004) and correlated with induction of metabolism via cytochrome P450 3A4. Importantly, the antibiotic, rifampin,

Correspondence: Professor NL Simmons, Epithelial Research Group, Institute for Cell and Molecular Biosciences, University of Newcastle Upon Tyne, Medical School, Framlington Place, Newcastle Upon Tyne NE2 4HH, UK.
E-mail: n.l.simmons@ncl.ac.uk
Received 25 September 2007; revised 14 December 2007; accepted 7 January 2008; published online 10 March 2008

has been identified as a potent and specific agonist of human PXR (Geick *et al*., 2001; Watkins *et al*., 2001). An important feature of PXR action is that of species differences and of differential regulation of gene activity in liver and intestine (Hartley *et al*., 2004). Activation of PXR by the antibiotic, rifampin, results in an increase in MDR1 expression and a subsequent reduction in the area under the plasma concentration curve for oral dosage of digoxin in humans (Drescher *et al*., 2003). This is of special significance, since digoxin displays a narrow therapeutic index (0.5–2 ng ml^{-1}).

Rifampin is not the only drug that may dynamically regulate MDR1 transcription. Takara *et al*. (2002, 2003a, b) have demonstrated that MDR1 mRNA expression is increased by digoxin itself, while concomitantly reducing PXR (SXR) mRNA levels. Digoxin oral doses are in the range 125–500 μg daily, so that luminal digoxin concentrations could routinely reach the micromolar range, leading to intestinal MDR1 induction and reduction in digoxin absorption. The exact mechanism by which digoxin exerts its influence on MDR1 expression levels remains uncertain.

Although a number of reports have investigated the regulation of efflux transport proteins by nuclear receptors, using various *in vitro* systems, most of these studies have reported changes in mRNA and protein expression levels as a measure for induction potential, without relating this to functional transport activity (Takara *et al*., 2002, 2003a, b). Those limited studies investigating the relationship between mRNA, protein levels and transport function (drug efflux), show contrasting results (Albertioni *et al*., 1995, Greiner *et al*., 1999, Taipalensuu *et al*., 2004).

It has long been recognized that the oral bioavailability of digoxin varies between 40 and 100% between individuals, but there have been surprisingly few studies aimed at investigating such variation (Mooradian, 1988). Clinical dosing of digoxin has recently undergone extensive review by the Digitalis Investigation Group, and as a result, lower dose digoxin therapy is now recommended to achieve a serum digoxin concentration in the range of 0.5 to 0.8 ng ml^{-1}, which has been associated with reduced mortality rates (Rathore *et al*., 2003). With such a narrow therapeutic window, a greater understanding of the mechanisms by which digoxin may be absorbed or excluded from the circulation, is essential.

Model systems of the human intestine, such as the Caco-2 cell line, although displaying MDR1 expression, are negative (or variable) with respect to PXR expression (Takara *et al*., 2003a, b; Li *et al*., 2007). Accordingly, we have screened other human cell lines for coexpression of MDR1 together with PXR and identified the human intestinal T84 cell line as positive for expression of both PXR and MDR1. T84 cells grown on permeable filter supports allow direct measurement of transepithelial solute fluxes, including those mediated by MDR1 (Hunter *et al*., 1991; Lowes and Simmons, 2002). Using the T84 cell system, we report activation by rifampin of MDR1 mRNA expression, and correlate this with functional assays of MDR1 transport using bidirectional [^{3}H]digoxin fluxes (Cavet *et al*., 1996; Lowes and Simmons, 2002). In addition, we have been able to compare the rifampin response of T84 cells to that seen after pre-exposure to digoxin. Whereas rifampin induction of MDR1 increased PXR transcription, digoxin induction of MDR1 functional activity was associated with both an increase in CAR expression and a marked reduction of PXR transcription.

Methods

Cell culture

All cell culture was performed in a class II laminar flow hood (Safeflow1.2; Bio Air Instruments, Siziano, Italy) under aseptic conditions. Caco-2 cells were maintained in high-glucose (4.5 g l^{-1} D-glucose) Dulbecco's modified Eagle's medium supplemented with foetal calf serum (10% v/v), L-glutamine (1 mM), non-essential amino acids (1% v/v) and the antibiotic gentamicin (30 μg ml^{-1}). LS180 and Calu-3 cells were maintained in minimum essential Eagle's medium supplemented with foetal calf serum (10% v/v), non-essential amino acids (1% v/v) and gentamicin (30 μg ml^{-1}). HT29 cells were maintained in RPMI 1640 supplemented with 10% (v/v) foetal calf serum in the presence of penicillin–streptomycin (5% v/v). HCT8 cells were maintained in RPMI 1640 supplemented with 10% (v/v) foetal calf serum, L-glutamine (1 mM) and sodium pyruvate (1 mM) in the presence of penicillin–streptomycin (5% v/v). T84 cells were supplied by AstraZeneca (Cheshire, UK) and used between passage numbers 6–15. Cells were maintained in a 1:1 mix of high-glucose (4.5 g l^{-1}) Dulbecco's modified Eagle's medium (Dulbecco's modified Eagle's medium) and HAMS F12 nutrient mixture, supplemented with foetal calf serum (10% v/v), HEPES (15 mM) and sodium pyruvate (1 mM). Cells were grown in the presence of an antibiotic mix of penicillin–streptomycin (5% v/v). T84 cells were seeded onto 12- or 96-well culture inserts (Transwell 3401 (12 mm diameter, 0.4 μm pore size, 1.14 cm2 growth area) and Transwell 3391 (4.26 mm diameter, 0.4 μm pore size, 0.11 cm2 growth area) uncoated polycarbonate filters; Costar, High Wycombe, UK) at high density (5×10^5 cells cm^{-2}). Cells were maintained at 37 °C in a humidified incubator with 5% CO_2 in air. Cells were allowed 7 days growth to confluence, as determined by measuring transepithelial electrical resistances (TEER) using a WPI EVOM voltohmeter (World Precision Instruments, Hertfordshire, UK).

Transepithelial transport experiments

Bidirectional transepithelial transport experiments using the MDR1 substrate digoxin were performed using T84 cells 7–10 days post-seeding. Prior to flux experiments, cells were pretreated with rifampin (0–10 μM), digoxin (100 nM or 1 μM) or the vehicle control, dimethyl sulphoxide (DMSO) (0.1% v/v) for between 0 and 96 h. All cell layers used in the time-course experiments were cultured for the same period of time. Upon reaching confluence, replacement medium containing either rifampin or an equivalent concentration of DMSO (0.1%) was added. Over the following days, the medium was replaced with or without drug (10 μM rifampin) as required. This was timed to ensure that [^{3}H]digoxin fluxes were measured on the same day, following identical culture time for each cell layer, regardless of drug treatment. This

ensured all cells were of the same age, with the only difference (apart from drug exposure) being the timing of medium replacements. All control layers were therefore of the same age as the treated layers, having been exposed to media containing DMSO (0.1%) as opposed to drug for the treatment period. It was determined previously that DMSO exposure (at 0.1%) had no impact on bidirectional digoxin fluxes.

Subsequent to treatment, T84 cell monolayers grown in 96-well Transwell plates were allowed a 3-h wash period in drug-free medium. Layers were then washed (three times) in Hank's buffered saline solution and placed in fresh 96-well base plates containing 200 μl Hank's buffered saline solution supplemented with 10 mM HEPES. Monolayers were allowed a 15-min equilibration period at 37 °C prior to TEER recordings.

For flux experiments, the buffer composition was identical for apical and basal compartments (Hank's buffered saline solution + 10 mM HEPES), with the addition of [^{3}H]digoxin (0.5 μCi ml^{-1}, total digoxin 0.1 μM) and [^{14}C]mannitol (0.1 μCi ml^{-1}, total concentration 100 μM) to either the apical or basal compartments.

Samples were taken to determine absorptive (apical-to-basal, J_{a-b}) and secretory (basal-to-apical, J_{b-a}) fluxes following a 1-h incubation at 37 °C. Flux calculations were performed as described previously (Cavet *et al*., 1996) and expressed as pmol cm^{-2} h^{-1}. Net secretion (J_{net}) was calculated from paired monolayers by subtracting apical-to-basal (J_{a-b}) from basal-to-apical (J_{b-a}) flux. Passive paracellular flux was determined by concurrent measurement of [^{14}C]mannitol movement. Mannitol is an inert sugar that is freely diffusable via the paracellular pathway. Movement of mannitol into the contralateral compartment was generally <2%. Monolayers in which contralateral mannitol movement was >3% were discounted from the results, based on compromised monolayer integrity.

For cells grown in 12-well Transwell plates, flux experiments were performed in an identical manner, except that a Krebs' buffer consisting of 137 mM NaCl, 5.4 mM KCl, 1 mM $MgSO_4$, 0.3 mM NaH_2PO_4, 0.3 mM KH_2PO_4, 10 mM glucose and 10 mM HEPES (buffered to pH 7.4 at 37 °C with Trizma base, with the addition of [^{3}H]digoxin 0.5 μCi ml^{-1} (total digoxin 1.0 μM)) and [^{14}C]mannitol (0.1 μCi ml^{-1}), total concentration 100 μM) to either the apical or basal compartments Samples were taken to determine transepithelial fluxes at 1, 2 and 3 h. To directly compare digoxin fluxes where different total digoxin concentrations were used and allow direct comparison with mannitol fluxes, permeabilities were calculated ($P_{b-a} = J_{b-a} \cdot C_b^{-1}$ or $P_{a-b} = J_{a-b} \cdot C_a^{-1}$), where P is the permeability in cm h^{-1}, J is the flux in pmol cm^{-2} h^{-1} and C_b and C_a represent concentrations of substrate in apical or basal compartments, respectively.

RNA isolation and RT-PCR

RNA was isolated from flasks confluent of epithelial cells using the Qiagen RNeasy mini-kit following the manufacturer's standard protocol. Reverse transcription of RNA (1 μg) used Omniscript reverse transciptase (Qiagen Ltd., Crawley, UK) according to the manufacturer's protocol. Hot-start *Taq* DNA polymerase (Qiagen) was used according to the manufacturer's protocol for amplification of 2 μl of reverse-transcribed RNA in a 50 μl reaction. Mg^{2+} concentration was 1.5 mM, primer concentration was 0.5 μM and 2.5 U of enzyme were used per reaction. Enzyme activation was achieved with an initial heating step of 95 °C for 15 min. The annealing temperature for all primer pairs was set at 54 °C. Amplification was carried out over 35 cycles. Gene-specific oligonucleotide primers for ABCB1 (MDR1), NR1I2 (PXR) and β-actin were designed from published human sequences (NCBI). Expected product sizes were 799 bp (ABCB1), 905 bp (NR1I2) and 605 bp (β-actin) (Table 1). Polymerase chain reaction (PCR) products were analysed by agarose gel (1%) electrophoresis, with products visualized using ethidium bromide staining and UV transillumination.

Table 1 Oligonucleotide primer pairs used for the identification of gene expression in human epithelial cell lines

Gene	*Sequence*	*Predicted size (bp)*
ABCB1 (MDR1)		
Forward	5′-GTGGGGCAAGTCAGTTCATT-3′	799
Reverse	5′-GCTCCTTGACTCTGCCATTC-3	
NR1I2 (PXR)		
Forward	5′-TGTATGTGGGGACAAGGC-3′	905
Reverse	5′-TCTGGGGAGAAGAGGGAG-3′	
β-Actin		
Forward	5′-TCCACGAAACTACCTTCAAC-3′	605
Reverse	5′-TTTAGGATGGCAAGGGAC-3′	

Abbreviations: ABCB1, ATP-binding cassette B1; MDR1, multi-drug resistance 1; PXR, pregnane X receptor.

Real-time quantitative PCR (TaqMan) analysis

To investigate the effect of rifampin and digoxin preincubation on MDR1, PXR and CAR mRNA expression, flasks were maintained in a manner identical to epithelial monolayers, with high-density seeding and culture for 7 days prior to experimentation. Total RNA was isolated as described above and contaminating DNA was digested with Turbo DNA-*free* (Ambion, Huntingdon, UK). RNA was quantified using a nanodrop ND-1000 spectrophotometer (Nanodrop Technologies Inc., Wilmington, DE, USA) and integrity was checked by measurement of the $A_{260/280\,nm}$ ratio, which was routinely in the range of 1.8 to 2. cDNA synthesis from 1 μg total RNA was performed using the SuperScript first-strand synthesis system (Invitrogen) according to the manufacturer's protocol. Product amplification by quantitative PCR was performed with 2 μl cDNA reaction, using quantitative PCR MasterMix plus Low ROX (Eurogentec, Southampton, UK) according to the manufacturer's guidelines. Negative controls involved omission of RNA from the reverse transcriptase (RT) reactions and amplification with specific primer/probe sets to confirm lack of genomic DNA contamination. Human genomic DNA was used to generate standard curves for each probe and primer set, allowing absolute quantification. Probes (Table 2) were labelled with 5′-FAM and 3′-DDQ1, purchased from Eurogentec. Amplification was performed over 40–50 cycles using the Stratagene

Table 2 Oligonucleotide primer and probe sets used for the amplification of gene expression in T84 cells

Gene	*Sequence*
ABCB1 (MDR1)	
Forward	5′-GTCCCAGGAGCCCATCCT-3′
Reverse	5′-CCCGGCTGTTGTCTCCATA-3′
Probe	5′-TTGACTGCAGCATTGCTGAGAACATTG C-3′
NR1I2 (PXR)	
Forward	5′-CGAGCTCCGCAGCATCA-3′
Reverse	5′-TGTATGTCCTGGATGCGCA-3′
Probe	5′-CGGTGCCATCCCTTGACTCAACCT-3′
NR1I3 (CAR)	
Forward	5′-CCAAATCCAGCACATCCAGG-3′
Reverse	5′-GCCTCAGCTGCAGATCTCCT-3′
Probe	5′-GTCTGCCATGATGCCGCTGCT-3′

Abbreviations: ABCB1, ATP-binding cassette B1; CAR, constitutive androstane receptor; MDR1, multi-drug resistance 1; PXR, pregnane X receptor.

MX4000. Data were normalized to the expression of 18S ribosomal RNA.

Western blotting

Total protein was extracted from confluent layers of T84 cells grown in 12-well plates (Corning) in a manner identical to epithelial monolayers, with high-density seeding and culture for 7 days prior to experimentation. Whole-cell lysis buffer consisted of 200 μl Igepal, 200 μl 10% sodium dodecyl sulphate, 10 μl 1 mM dithiothreitol and 9.59 ml phosphate-buffered saline, with addition of 1 × protease inhibitor cocktail tablet (Roche, Welwyn Garden City, UK). Protein was quantified using Bradford reagent (Bio-Rad, Hemel Hempstead, UK). Proteins were separated on 8% sodium dodecyl sulphate–polyacrylamide gels and transferred onto polyvinylidene difluoride membranes (Millipore, Consett, UK) overnight. Membranes were washed briefly with TBS-T (Tris-buffered saline and 0.1% Tween-20, pH 7.6) and blocked in 3% non-fat dried milk in TBS-T buffer. Membranes were probed overnight at 4 °C with the mouse monoclonal antibody C219 (Calbiochem, Nottingham, UK) directed against an internal epitope of human MDR1. The antibody was diluted 1:50 in TBS-T buffer. Following further washing, membranes were incubated with HRP-labelled anti-mouse IgG (Abcam, Cambridge, UK) and bands were detected with the pico-chemiluminescence substrate (Pierce, Cramlington, UK) following the manufacturer's instructions.

Equal loading was confirmed by re-probing blotted membrane for β-actin. Membranes were stripped and washed with TBS-T. They were probed with the mouse anti-human β-actin antibody (Abcam) diluted 1:100 in 5% milk (in TBS-T buffer). Secondary staining and chemiluminescence were performed as described previously.

Immunocytochemistry and confocal microscopy

T84 cell monolayers were grown on 12-well permeable culture inserts (Transwell 3401, 12 mm diameter, 0.4 μm pore size, uncoated polycarbonate filters; Costar) until confluence. Layers used to detect altered P-glycoprotein expression were incubated for 72 h with the vehicle (0.1% DMSO), rifampin (10 μM) or digoxin (1 μM). Cells were fixed with 100% methanol (MeOH) for occludin staining or with 3% paraformaldehyde for P-glycoprotein staining. Paraformaldehyde-fixed cells were permeabilized with 0.1% Triton X. Filters were cut from the inserts and following non-specific blocking with 3% (v/v) donkey serum, cells were probed using mouse monoclonal anti-occludin antibody at a dilution of 1:100 (Calbiochem), or with mouse antibody UIC2 (directed against an extracellular conformational epitope of MDR1) at 1:50 (Chemicon). Secondary block was performed with goat serum and secondary detection was with goat anti-mouse Alexa-Fluor 488, at 1:100. Negative control experiments omitted the primary antibody and were negative for any specific fluorescence. Concurrent nuclear staining was performed using propidium iodide at 1:1000.

Cells were imaged by confocal laser scanning microscopy (TCS-NT; with Kr–Ar laser; Leica, Milton Keynes, UK) using appropriate excitation and emission filter sets for dual fluorophore detection and a 63 × HCX PL APO objective with a numerical aperture of 1.4 giving optical sections of $>0.4\,\mu m$.

Statistics

Results are expressed as mean ± s.e.mean (n). For statistics relating to J_{net}, individual values of net flux from paired monolayers were used. Statistical analysis was performed using Student's unpaired t-tests or one-way analysis of variance, with Bonferroni's *post test* for multiple comparisons (GraphPad Instat, San Diego, CA, USA).

Materials

[^{14}C]Mannitol (specific activity 56 mCi mmol^{-1}) and [^{3}H]digoxin (specific activity 21.8 Ci mmol^{-1}) were obtained from PerkinElmer (Boston, MA, USA), cell culture medium and supplements were from Sigma (Poole, Dorset, UK) and tissue culture plastic flasks and culture plates were supplied by Costar. All other chemicals were obtained from Sigma.

Results

Expression of MDR1 and PXR mRNA in cultured epithelial cells

Coexpression of MDR1 and PXR mRNA was investigated by RT-PCR in a number of epithelial cell lines (Figure 1). MDR1 expression was confirmed in the intestinal Caco-2, HCT8, T84 and LS180 cell lines and faintly detectable in the respiratory Calu-3 cell line, with each displaying a PCR product of the expected size (799 bp). MDR1 expression was not detectable in the intestinal HT29 cell line. PXR expression was restricted to the T84 and LS180 cell lines (Figure 1b, expected product size 905 bp). PXR mRNA levels were below the level of detection in the Caco-2, Calu-3, HT29 and HCT8 cell lines. Since LS180 intestinal cells do not reconstitute epithelial layers on permeable filters, the T84 cell line was selected for further studies.

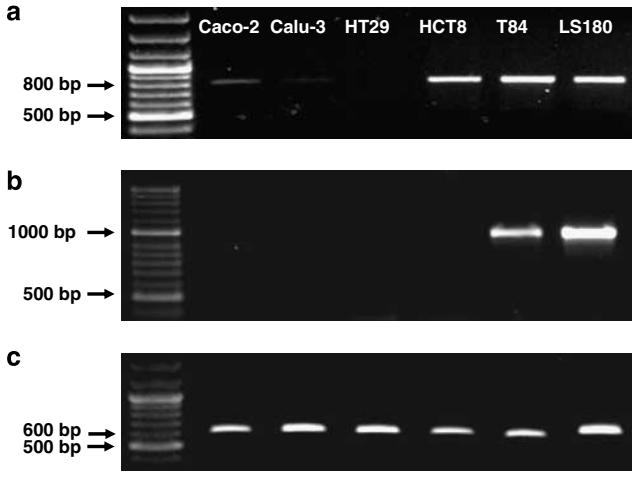

Figure 1 Ethidium bromide-stained agarose gels of RT-PCR products from the human Caco-2, Calu-3, HT29, HCT8, T84 and LS180 epithelial cell lines. (**a**) RT-PCR products obtained using ABCB1 (MDR1)-specific primers (product size of 799 bp). (**b**) RT-PCR products obtained using NR1I2 (PXR)-specific primers (expected product size of 905 bp). (**c**) RT-PCR products obtained using β-actin-specific primers (expected product size of 605 bp). See Table 1 for forward and reverse primer sequences. RT-PCR, reverse transcription-polymerase chain reaction.

Effects of rifampin and digoxin pretreatment on transepithelial digoxin fluxes in the T84 epithelia

Figure 2 shows digoxin secretion in T84 control layers as expected from MDR1 mRNA expression; control basal-to-apical J_{b-a} [^{3}H]digoxin flux rates are maintained up to 3 h at a constant level and exceed absorptive apical-to-basal (J_{a-b}) fluxes. Net secretory digoxin flux (J_{b-a}–J_{a-b}) was increased following 72 h pretreatment with 10 μM rifampin (Figures 2 and 3a). This increase was primarily due to an increase in J_{b-a} Expressing this as changes in permeability, the control secretory permeability ($P_{\mathrm{b\text{-}a}} = 3.5 \pm 0.2 \times 10^{-2}\,\mathrm{cm\,h^{-1}}$) was raised to $5.9 \pm 0.02 \times 10^{-2}\,\mathrm{cm\,h^{-1}}$ after rifampin treatment, $n = 6$; $P < 0.001$), but rifampin also reduced absorptive permeability ($P_{\mathrm{a-b}} = 0.7 \pm 0.1 \times 10^{-2}\,\mathrm{cm\,h^{-1}}$ in controls to $0.4 \pm 0.0(3) \times 10^{-2}\,\mathrm{cm\,h^{-1}}$ with rifampin treatment, $n = 6$; $P < 0.05$; Figure 2). Increases in net digoxin secretion following 72 h preincubation were not only observed with rifampin (Figure 3a), but also after preincubation with 100 nM digoxin (control secretory permeability, $P_{\mathrm{b-a}}$, measured using 100 nM digoxin, $3.5 \pm 0.2 \times 10^{-2}\,\mathrm{cm\,h^{-1}}$ compared with $4.3 \pm 0.1 \times 10^{-2}\,\mathrm{cm\,h^{-1}}$ 100 nM digoxin treated, $n = 6$; $P < 0.05$; Figure 3b) and 1 μM digoxin (control permeability, $2.8 \pm 0.1 \times 10^{-2}$ and $4.95 \pm 0.15 \times 10^{-2}\,\mathrm{cm\,h^{-1}}$, 1 μM digoxin treated, $n = 6$; $P < 0.05$; Figure 3c). As with rifampin, digoxin preincubation increased net digoxin secretion due to an increase in basal to apical (J_{b-a}) digoxin flux (Figures 3b and c). Absorptive digoxin permeability ($P_{\mathrm{a-b}}$) was slightly increased at 100 nM ($0.6 \pm 0.0(4) \times 10^{-2}\,\mathrm{cm\,h^{-1}}$ control and $0.7 \pm 0.0(2) \times 10^{-2}\,\mathrm{cm\,h^{-1}}$ digoxin; Figure 3b, $n = 6$; $P < 0.05$) and 1 μM digoxin ($0.50 \pm 0.0(2) \times 10^{-2}\,\mathrm{cm\,h^{-1}}$ control and $0.8 \pm 0.1\,\mathrm{cm\,h^{-1}} \times 10^{-2}$ digoxin; Figure 3c, $n = 6$; $P < 0.05$) preincubations. The increase in absorptive digoxin transport correlated with TEER measurements following treatment; whereas rifampin pretreatment was without effect (control

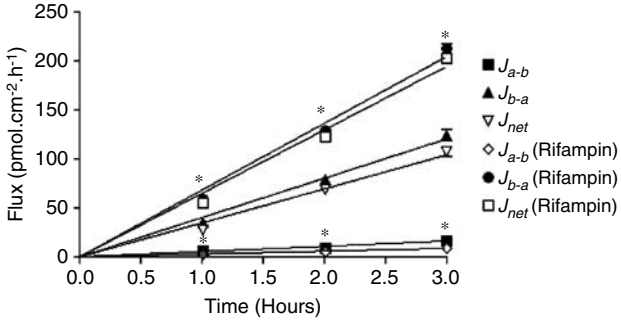

Figure 2 Bidirectional transepithelial [^{3}H]digoxin fluxes across confluent monolayers of T84 cells grown in the presence or absence of 10 μM rifampin for 72 h exposure. [^{3}H]digoxin (0.5 μCi ml^{-1}, total digoxin 1 μM) fluxes were determined up to 3 h either in the apical-to-basal (J_{a-b}) or basal-to-apical (J_{b-a}) directions. Net secretion (basal to apical), $J_{net} = J_{b-a} - J_{a-b}$. *Significantly different from control values (0.1% DMSO vehicle); $P < 0.05$. Data are expressed as ± s.e.mean, $n = 6$ replicates from an individual experiment. DMSO, dimethyl sulphoxide.

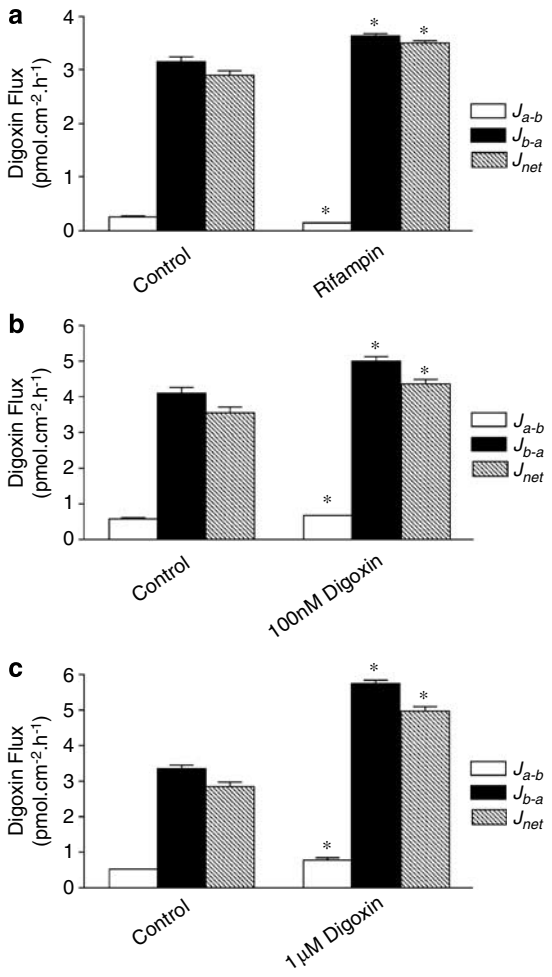

Figure 3 Comparison of the effect of rifampin and digoxin preincubation upon transepithelial [^{3}H]digoxin (0.5 μCi ml^{-1}, total digoxin 100 nM) fluxes across confluent monolayers of T84 cells. Fluxes were determined over 1 h (as in Figure 2) following 72 h incubation with 10 μM rifampin (**a**), 100 nM digoxin (**b**) and 1 μM digoxin (**c**). *Significantly different from controls (0.1% DMSO vehicle); $P < 0.05$. Data are expressed as ± s.e.mean, $n = 6$ replicates from an individual experiment. DMSO, dimethyl sulphoxide.

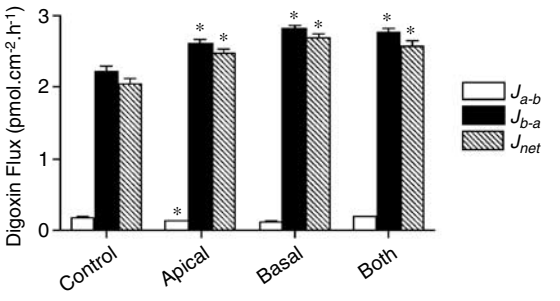

Figure 4 Effects of exposure to 10 μM rifampin from either the apical or basolateral membranes on transepithelial [^{3}H]digoxin (0.5 μCi ml^{-1} total digoxin 1 μM) fluxes. Apical-to-basal (J_{a-b}) and basal-to-apical (J_{b-a}) and net fluxes ($J_{net}=J_{b-a}-J_{a-b}$) (determined as in Figure 2) following 72 h exposure to 10 μM rifampin from either the apical or basolateral surfaces alone, or both surfaces concurrently. *Significantly different from control values; $P<0.05$. Data are expressed as ± s.e.mean, $n=6$ replicates from an individual experiment.

TEER, 1137 ± 46 Ωcm^2; plus rifampin, 1266 ± 39 Ω cm^2, NS, $n=12$), digoxin pretreatment reduced TEER (726 ± 14 Ω cm^2 control to 279 ± 11 Ω cm^2, 100 nM digoxin, and 944 ± 18 Ω cm^2 control to 99 ± 5 Ωcm^2, 1 μM digoxin, $n=12$; $P<0.05$). Similarly, the concurrently measured values of transepithelial mannitol permeability were unaltered by rifampin treatment ($0.1(4)\pm0.1\times10^{-2}$ cm h^{-1}, control; $0.1\pm0.0(4)\times10^{-2}$ cm h^{-1}, 10 μM rifampin), but increased by digoxin ($0.3\pm0.0(2)\times10^{-2}$ cm h^{-1}, control; $0.5\pm0.0(2)\times10^{-2}$ cm h^{-1}, 100 nM digoxin and $1.4\pm0.1\times10^{-2}$ cm h^{-1}, 1 μM digoxin, $n=12$; both $P<0.05$). This indicates that long-term digoxin pretreatment resulted in increased paracellular permeability. The increase in the subsequently measured digoxin basal-to-apical flux (J_{b-a}) was such that the efflux ratio for digoxin (J_{b-a}/J_{a-b}) was maintained despite increase in paracellular permeability.

Figure 4 shows that exposure of either epithelial surface to 10 μM rifampin was sufficient to stimulate net transepithelial [^{3}H]digoxin fluxes; a 72-h exposure to rifampin from either the apical or basolateral surfaces produced increments in net flux compared with control values. Rifampin may therefore gain access to cellular nuclear receptors from the luminal compartment alone.

Comparison of rifampin and digoxin pretreatment effect on net digoxin flux and MDR1 mRNA levels

As rifampin is a specific PXR agonist, activation of digoxin transport should be correlated with increased MDR1 mRNA expression. Quantitative real-time PCR was performed to determine changes in MDR1 mRNA expression levels following rifampin and digoxin treatments (Figure 5b). After 72 h of rifampin pretreatment, a threefold increase in MDR1 transcript level was observed (Figure 5b, $n=4$; $P<0.05$), which correlated with increased net digoxin flux (Figure 5a, $n=6$; $P<0.05$). In contrast, digoxin pretreatment displayed far greater increase in MDR1 mRNA levels at 100 nM or 1 μM concentration($n=4$; $P<0.05$; Figure 5b). These marked increases in MDR1 gene expression correlated with relatively small increases in net digoxin transport after 100 nM and 1 μM digoxin pretreatments ($n=6$; $P<0.05$; Figure 5a). It was

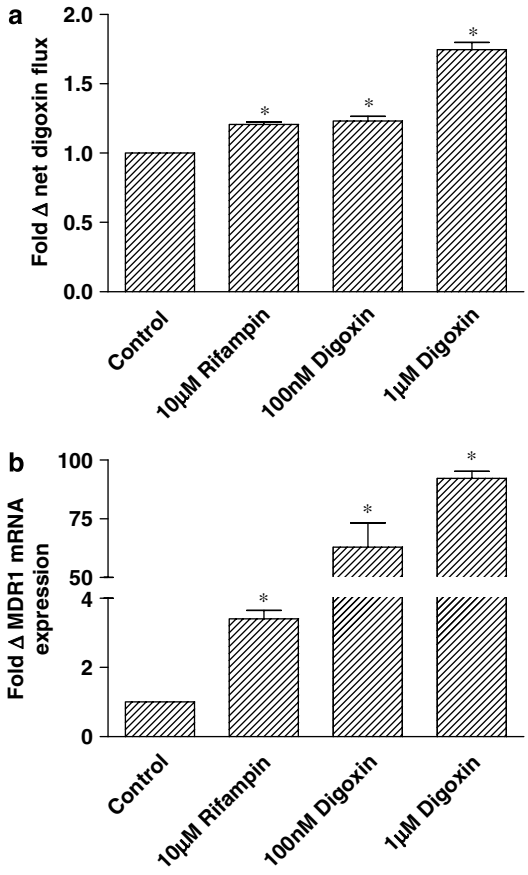

Figure 5 Comparison of MDR1 mRNA expression to digoxin transport. Confluent monolayers of T84 cells were treated for 72 h with 10 μM rifampin and 100 nM and 1 μM digoxin. (**a**) Fold changes in net [^{3}H]digoxin flux were calculated in relation to control values. Significant increases in net flux were observed following both rifampin and digoxin treatments ($P<0.05$, $n=6$ replicates from individual experiments). (**b**) Fold changes in MDR1 (ABCB1) mRNA expression were determined by TaqMan analysis following amplification using gene-specific primers and probes (see Table 2). *Significantly different from control values; $P<0.05$. Data are expressed as ± s.e.mean, $n=4$ replicate wells. ABCB1, ATP-binding cassette B1; MDR1, multidrug resistance 1.

therefore clear that there was no fixed relationship between MDR1 transcript level and functional activity.

Comparison of rifampin and digoxin pretreatment effect on PXR and CAR mRNA levels

Pregnane X receptor and CAR mRNA levels were assessed to determine the stability of nuclear receptor expression during pretreatments (Figure 6). Whereas rifampin incubations increased PXR mRNA twofold (Figure 6a, $n=4$; $P<0.05$), digoxin preincubations resulted in substantial drops in PXR expression levels with either 100 nM or 1 μM digoxin (Figure 6a, $n=4$; $P<0.05$). The opposite effects of digoxin treatment on MDR1 and PXR mRNA expression are in agreement with the results reported by Takara *et al*. (2003a) in Caco-2 cells expressing variable PXR levels. The impact on CAR transcript levels was different. Rifampin incubation resulted in a greater increase in CAR expression (Figure 6b, $n=4$; $P<0.05$) than was seen for PXR. Whereas digoxin

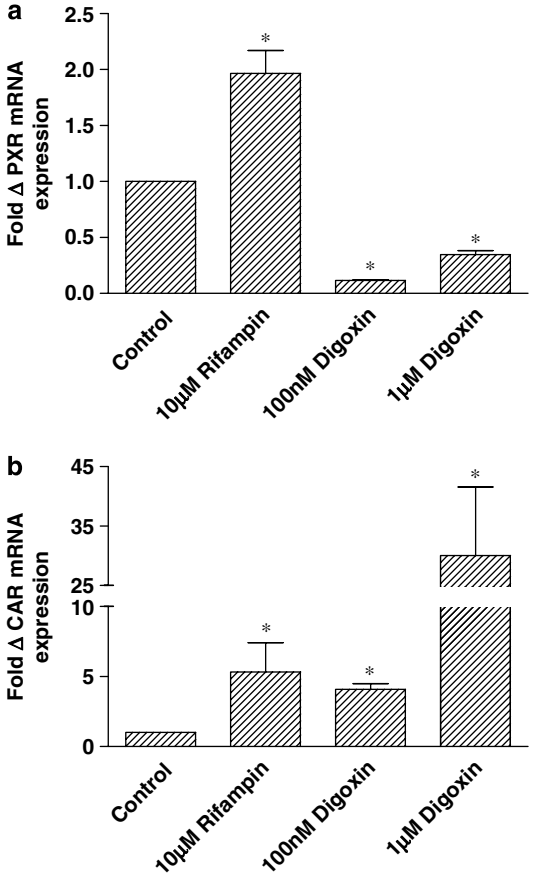

Figure 6 Fold changes in (**a**) PXR (NR1I2) and (**b**) CAR (NR1I3) mRNA expression were determined by TaqMan analysis following amplification using gene-specific primers and probes (see Table 2). Transcript levels in confluent monolayers of T84 cells were determined following 72 h of treatment with 10 μM rifampin and 100 nM and 1 μM digoxin. *Significantly different from control values; $P<0.05$. Data are expressed as ± s.e.mean, $n=4$ separate wells. CAR, constitutive androstane receptor; PXR, pregnane X receptor.

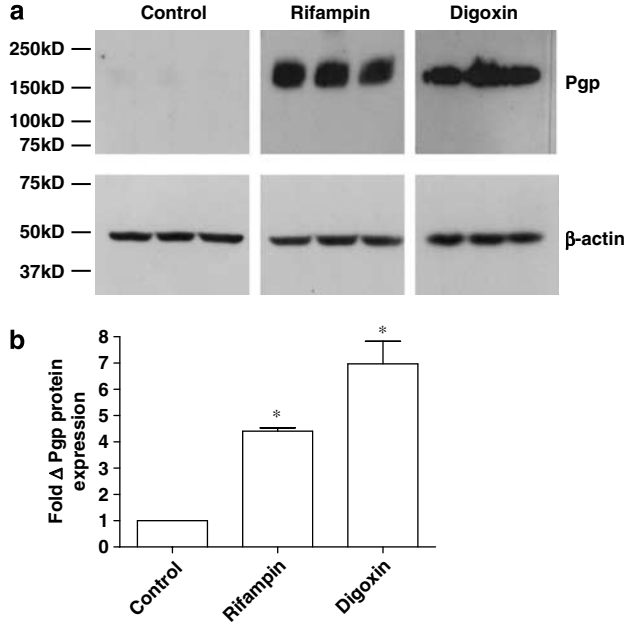

Figure 7 (**a**) Western blot analysis of MDR1 protein expression in T84 cell monolayers following 72 h of exposure to rifampin (10 μM) and digoxin (1 μM). A 50-μg weight of control (0.1% DMSO) and rifampin-treated protein, and 25 μg of digoxin-treated T84 protein was loaded into each lane, with bands representing protein from three separate cell layers for each condition. (**b**) Band intensity was determined by densitometry and normalized to β-actin protein levels. *Significantly different from control values; $P<0.05$. Data are expressed as ± s.e.mean, $n=3$ samples. DMSO, dimethyl sulphoxide; MDR1, multidrug resistance 1.

reduced PXR expression, CAR mRNA levels were increased following 100 nM or 1 μM digoxin treatment, (Figure 6b, $n=4$; $P<0.05$).

Effects of rifampin and digoxin treatment on MDR1 protein expression and localization in T84 cells

Western blot analysis and immunocytochemistry were used to determine the impact of rifampin and digoxin on protein expression and localization in T84 cells. MDR1 protein expression was detectable in control cells (note that a limited 30-min film exposure was used for comparative purposes) (Figure 7); pretreatment with 10 μM rifampin markedly increased protein expression (the data in Figure 7 are from three separate protein extractions from the same passage of T84 cells). Densitometric analysis, normalized to β-actin loading controls, indicated a fourfold increase in MDR1 expression ($n=3$; $P<0.05$) following rifampin (10 μM) pretreatment. This increase in protein expression following rifampin treatment is of an order similar to that seen for MDR1 mRNA (3.4-fold), but exceeds that for functional activity (1.2-fold). Digoxin pretreatment (1 μM) also significantly increased MDR1 expression ($n=3$; $P<0.05$; Figure 7). The digoxin-induced protein increase displays a far smaller increase than that of MDR1 transcript levels (92-fold), but is still substantially higher than the increase measured in functional activity (1.75-fold). Taken together, these data suggested that functional activity might be determined by the cellular localization of the protein.

Figure 8 shows MDR1 localization using the UIC2 antibody after fixation and permeabilization. It can be seen that under control conditions, expression is limited to a distinct sub-population of cells. Vertical optical sectioning (*x–z*) of the cell monolayer confirms confluence of the monolayer and together with optical sections at the apical surface (*x–y*) the predominately apical (brush border) expression of MDR1 in these cells. Comparative images for the apical tight-junctional protein occludin (Furuse *et al*., 1993; Figure 8d) are shown for comparison. Following rifampin (10 μM) treatment, the number of cells showing apical (brush border) staining of MDR1 increased dramatically. Further increases in the number of cells expressing MDR1 were seen following digoxin treatment, with the entire monolayer appearing to display some degree of expression, as cell boundaries are not visible. Measurement of integrated pixel intensity in optical sections of the brush-border in the three conditions showed that rifampin treatment increased apical MDR1 levels by 2.7 ± 0.5-fold ($n=6$; $P<0.05$; Figure 8b), whereas digoxin treatment increased apical MDR1 levels by 4.7 ± 0.5(5)-fold ($n=6$; $P<0.05$; Figure 8c).

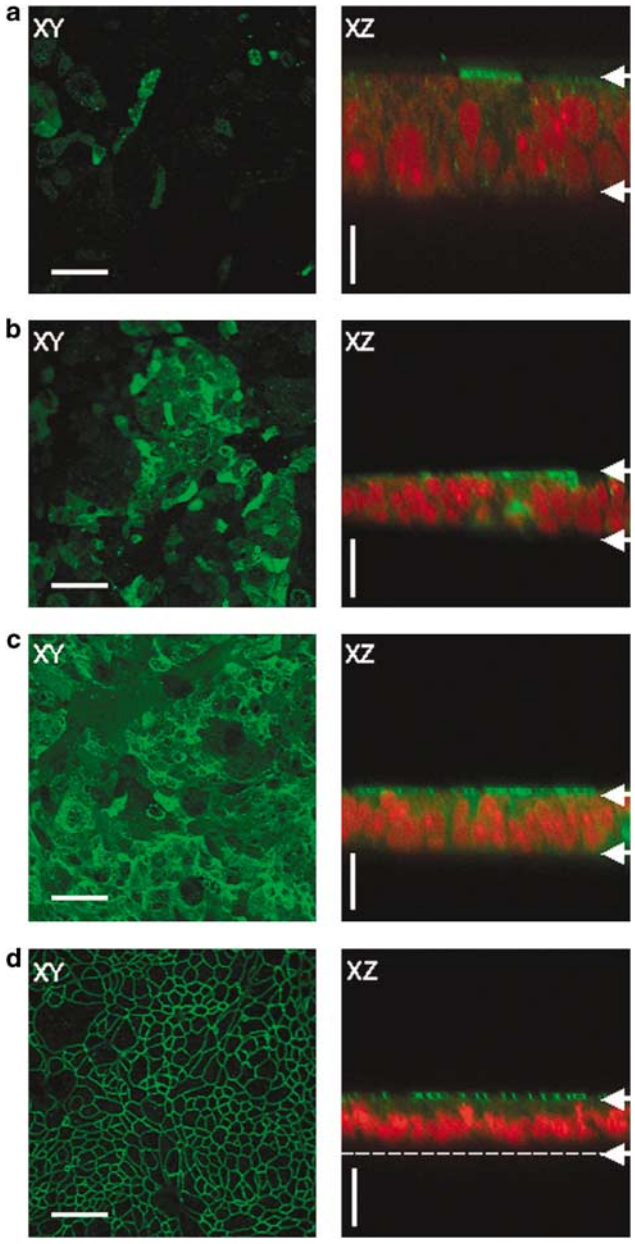

Figure 8 Cellular localization of MDR1 by immunocytochemistry. UIC2/goat anti-mouse Alexa-Fluor 488 immunofluorescence (green) and propidium iodide fluorescence (red) visualized by laser-scanning confocal microscopy in control (0.1% DMSO) (**a**), rifampin (10 μM) (**b**) and 72-h digoxin-treated (1 μM) (**c**) T84 cell monolayers grown on permeable Transwell supports. (**d**) Occludin/goat anti-mouse Alexa-Fluor 488 immunofluorescence (green) and propidium iodide fluorescence (red). *x–y* images display horizontal confocal optical section at the level of the apical cell surface, whereas *x–z* images show vertical optical cross-sections of the epithelial monolayer. Arrows indicate the apical surface (upper) or basal cell/filter border (lower). Note the columnar morphology and prominent nuclei (propidium staining). Representative images from three experiments. Scale bars: (*x–y*, **a–d**) = 20 μm; (*x–z*, **a**) = 10 μm and (*x–z*, **b–d**) = 20 μm.

Discussion

The ability of a wide range of xenobiotics to upregulate the expression of MDR1 both *in vitro* and *in vivo* is now well established (Geick *et al*., 2001; Maglich *et al*., 2002; Romiti *et al*., 2002). Rifampin, an antibiotic used to treat leprosy and tuberculosis, leads to induction of MDR1, resulting in clinically important drug–drug interactions (Greiner *et al*., 1999; Westphal *et al*., 2000; Drescher *et al*., 2003). Induction by rifampin is mediated via PXR, since rifampin is a specific agonist for this member of the NR1I family of nuclear receptors (Moore *et al*., 2000). This study has identified a model human intestinal cell line, T84, that coexpresses both PXR and MDR1. Reconstitution of the epithelial monolayers of T84 cells allows functional characterization of MDR1 activity by measurement of the fluxes of the model substrate [^{3}H]digoxin. Rifampin was found to increase MDR1 mRNA, MDR1 protein and transepithelial digoxin secretion. T84 cells express vasoactive intestinal peptide-stimulated anion secretion, and are so thought to represent a colonic crypt phenotype (Madara *et al*., 1987). At present it is unknown whether, *in vivo*, alterations in MDR1 levels occur first in the crypt cell population and are subsequently maintained during migration and differentiation towards the villus tip.

In a previous study in which functional induction of MDR1 activity was assessed after hyperforin treatment (Tian *et al*., 2005), a good correlation was found between the measured increase in cellular digoxin efflux rate constant and MDR1 protein. In the T84 model system, the relationship between rifampin-stimulated increases in transcript, protein and functional activity does not appear to be strictly linear with larger increases in mRNA (~3.4-fold) and protein levels (~4.4-fold) compared with functional activity (~1.2-fold), as determined by digoxin secretory transport at 72 h. Immunocytochemical localization of MDR1 in T84 cell monolayers after rifampin induction shows an increase in the number of cells displaying apical expression of MDR1 (Figure 8b), which correlates with the overall increase in protein expression. Endocytic trafficking and recycling of MDR1 in clathrin-coated pits has previously been reported in cancer cell lines (Kim *et al*., 1997) to represent a mechanism for changes in MDR1 levels at the plasma membrane, independent of nuclear receptor involvement, but this can only represent a minor component judging by the immunocytochemical data presented here. Since transepithelial transport must occur across both the basolateral and apical membranes in series, one possibility for the attenuated response of transport compared with protein in T84 epithelial layers is that delivery of digoxin substrate across the basolateral membrane is not subject to PXR-mediated induction. In rat, activators of PXR stimulate the expression of OATP2 (a high-affinity digoxin transporter) in liver but not in the intestine (Hartley *et al*., 2004). The increase in cells expressing MDR1 could arise from cell division of cells that were MDR1 positive. Since the mitotic index in confluent T84 cultures is very low, as judged by the number of mitotic figures, it seems more likely that induction occurs within cells expressing PXR, but with a low MDR1 expression level.

Here it is demonstrated that low and sub-micromolar concentrations of digoxin markedly increase MDR1 mRNA and protein expression in the human intestinal epithelial cell line T84, resulting in enhanced secretory transport of digoxin by these intestinal cells. With 1 μM of digoxin, the increase in MDR1 mRNA and protein levels exceeds that seen

for rifampin induction. This suggests that prolonged dosage with digitalis will result in upregulation of MDR1 and decreased oral bioavailability reducing plasma concentrations. It is less certain whether digoxin upregulation of MDR1 mRNA expression, protein and transport is mediated by an interaction with PXR. The suprising result that digoxin results in a marked reduction in PXR mRNA with simultaneous increases in CAR mRNA expression, suggests that an alternative nuclear receptor pathway may exist. Studies of digoxin upregulation of MDR1 activity in PXR-expressing Caco-2 cells also show marked downregulation of PXR mRNA expression (Takara *et al*., 2003a), suggesting that this is a common feature of the response of intestinal cells to digoxin. Regulation of MDR1 expression is not exclusively controlled by PXR and it is now recognized that CAR also exerts transcriptional control over the ABC transporter (Maglich *et al*., 2002; Burk *et al*., 2005; Cerveny *et al*., 2007). Although PXR and CAR share a number of common ligands (Maglich *et al*., 2002), rifampin has been confirmed to act through PXR alone (Moore *et al*., 2000). However, it is less certain whether the changes in MDR1, PXR and CAR expression following digoxin exposure result from the activation of PXR or another nuclear receptor. There have been conflicting reports surrounding the ability of CAR to regulate PXR levels (Maglich *et al*., 2002; Gibson *et al*., 2006). Recently it has been reported that co-transfection of CAR in Huh7 cells resulted in downregulation of PXR expression, as determined by reporter gene assay (Gibson *et al*., 2006). Without conducting assays involving reporter gene contructs, this study cannot evaluate interactions between digoxin and CAR.

Upregulation of MDR1 has also been reported to occur following toxic insult, resulting in a complex signalling cascade, which includes amongst others, activation of nuclear factor κB (NF-κB), a key regulator of inflammatory and immune responses (Thevenod and Friedmann, 1999; Kuo *et al*., 2002; Zhou *et al*., 2006). NF-κB is a transcription factor, held in the cytoplasm under non-stimulated conditions and released upon phosphorylation of IκB (inhibitor of NF-κB). Interestingly, Zhou *et al*. (2006) reported a reciprocal inhibitory cross-talk between PXR and NF-κB. PXR activation by rifampin antagonized NF-κB signalling, resulting in downregulation of certain NF-κB target genes (for example, TNFα). Likewise, activation of NF-κB resulted in attenuated PXR activity with reduced expression of the target gene cytochrome P450 3A4 (Zhou *et al*., 2006). It therefore appears that toxic insult can increase MDR1 expression through PXR- and CAR-independent mechanisms, and this may explain the distinct expression characteristics resulting from rifampin and digoxin exposure. As T84 cells exposed to digoxin show signs of toxicity (demonstrated by increased paracellular flux of mannitol and reduced TEER), the activation of NF-κB may participate in increasing MDR1 expression in this system. At present, however, this study can provide no conclusive evidence as to which transcription factor plays the dominant role in altered gene transcription in response to digoxin treatment.

In conclusion, this study has described the use of an *in vitro* human intestinal cell system, T84, for modelling PXR-mediated regulation of MDR1 function. A comparison with digoxin regulation of MDR1-mediated transport has disclosed distinct differences from rifampin regulation, on the basis of the observed depression of PXR mRNA expression. This may suggest alternative pathways for regulation of MDR1 expression by different xenobiotics. The result is also significant in terms of oral digoxin dosing, suggesting that chronic treatment regimes may increase MDR1 expression, reducing circulatory digoxin concentration and effecting therapeutic efficacy. Regular monitoring of digoxin plasma concentration would therefore be recommended to maintain dose within the therapeutic range (0.5–0.8 ng ml^{-1}).

Acknowledgements

We are grateful to Clare Summers at AstraZeneca for support with TaqMan analysis. TaqMan probe and primer sequences were kindly supplied by Katherine Howe (University of Surrey). This work was supported by a BBSRC CASE studentship award in conjunction with AstraZeneca.

Conflict of interest

The authors state no conflict of interest.

References

Albertioni F, Gruber A, Arestrom I, Vitols S (1995). Multidrug resistance gene (mdr1) RNA levels in relation to P-glycoprotein content of leukemic cells from patients with acute leukemia. *Med Oncol* **12**: 79–86.

Allen JD, Van Loevezijn A, Lakhai JM, Van Der Valk M, Van Tellingen O, Reid G *et al*. (2002). Potent and specific inhibition of the breast cancer resistance protein multidrug transporter *in vitro* and in mouse intestine by a novel analogue of fumitremorgin C. *Mol Cancer Ther* **1**: 417–425.

Burk O, Arnold KA, Geick A, Tegude H, Eichelbaum M (2005). A role for constitutive androstane receptor in the regulation of human intestinal MDR1 expression. *Biol Chem* **386**: 503–513.

Cavet ME, West M, Simmons NL (1996). Transport and epithelial secretion of the cardiac glycoside, digoxin, by human intestinal epithelial (Caco-2) cells. *Br J Pharmacol* **118**: 1389–1396.

Cerveny L, Svecova L, Anzenbacherova E, Vrzal R, Staud F, Dvorak Z *et al*. (2007). Valproic acid induces CYP3A4 and MDR1 gene expression by activation of constitutive androstane receptor and pregnane X receptor pathways. *Drug Metab Dispos* **35**: 1032–1041.

Drescher S, Glaeser H, Murdter T, Hitzl M, Eichelbaum M, Fromm MF (2003). P-glycoprotein-mediated intestinal and biliary digoxin transport in humans. *Clin Pharmacol Ther* **73**: 223–321.

Furuse M, Hirase T, Itoh M, Nagafuchi A, Yonemura S, Tsukita S *et al*. (1993). Occludin: a novel integral membrane protein localizing at tight junctions. *J Cell Biol* **123**: 1777–1788.

Geick A, Eichelbaum M, Burk O (2001). Nuclear receptor response elements mediate induction of intestinal MDR1 by rifampin. *J Biol Chem* **276**: 14581–14587.

Gibson GG, Phillips A, Aouabdi S, Plant K, Plant N (2006). Transcriptional regulation of the human pregnane-X receptor. *Drug Metab Rev* **38**: 31–49.

Greiner B, Eichelbaum M, Fritz P, Kreichgauer HP, Von Richter O, Zundler J *et al*. (1999). The role of intestinal P-glycoprotein in the interaction of digoxin and rifampin. *J Clin Invest* **104**: 147–153.

Hartley DP, Dai X HE YD, Carlini EJ, Wang B, Huskey SE, Ulrich RG *et al*. (2004). Activators of the rat pregnane X receptor differentially modulate hepatic and intestinal gene expression. *Mol Pharmacol* **65**: 1159–1171.

Hunter J, Hirst BH, Simmons NL (1991). Epithelial secretion of vinblastine by human intestinal adenocarcinoma cell (HCT-8 and T84) layers expressing P-glycoprotein. *Br J Cancer* **64**: 437–444.

Hunter J, Jepsom MA, Tsuruo T, Simmons NL, Hirst BH (1993). Functional expression of P-glycoprotein in apical membranes of human intestinal Caco-2 cells. Kinetics of vinblastine secretion and interaction with modulators. *J Biol Chem* **268**: 14991–14997.

Jonker JW, Buitelaar M, Wagenaar E, Van Der Valk MA, Scheffer GL, Scheper RJ *et al.* (2002). The breast cancer resistance protein protects against a major chlorophyll-derived dietary phototoxin and protoporphyria. *Proc Natl Acad Sci USA* **99**: 15649–15654.

Kim H, Barroso M, Samantha R, Greenberger L, Sztul E (1997). Experimentally induced changes in the endocytic traffic of P-glycoprotein alter drug resistance of cancer cells. *Am J Physiol* **273**: C687–C702.

Kuo MT, Liu Z, Wei Y, Lin-Lee YC, Tatebe S, Mills GB *et al.* (2002). Induction of human MDR1 gene expression by 2-acetylaminofluorene is mediated by effectors of the phosphoinositide 3-kinase pathway that activate NF-kappaB signaling. *Oncogene* **21**: 1945–1954.

Li T, Chen W, Chiang JY (2007). PXR induces CYP27A1 and regulates cholesterol metabolism in the intestine. *J Lipid Res* **48**: 373–384.

Lowes S, Simmons NL (2002). Multiple pathways for fluoroquinolone secretion by human intestinal epithelial (Caco-2) cells. *Br J Pharmacol* **135**: 1263–1275.

Luo G, Cunningham M, Kim S, Burn T, Lin J, Sinz M *et al.* (2002). CYP3A4 induction by drugs: correlation between a pregnane X receptor reporter gene assay and CYP3A4 expression in human hepatocytes. *Drug Metab Dispos* **30**: 795–804.

Luo G, Guenthner T, Gan LS, Humphreys WG (2004). CYP3A4 induction by xenobiotics: biochemistry, experimental methods and impact on drug discovery and development. *Curr Drug Metab* **5**: 483–505.

Madara JL, Stafford J, Dharmsathaphorn K, Carslon S (1987). Structural analysis of a human intestinal epithelial cell line. *Gastroenterology* **92**: 1133–1145.

Maglich JM, Stoltz CM, Goodwin B, Hawkins-Brown D, Moore JT, Kliewer SA (2002). Nuclear pregnane x receptor and constitutive androstane receptor regulate overlapping but distinct sets of genes involved in xenobiotic detoxification. *Mol Pharmacol* **62**: 638–646.

Mooradian AD (1988). Digitalis. An update of clinical pharmacokinetics, therapeutic monitoring techniques and treatment recommendations. *Clin Pharmacokinet* **15**: 165–179.

Moore LB, Parks DJ, Jones SA, Bledsoe RK, Consler TG, Stimmel JB *et al.* (2000). Orphan nuclear receptors constitutive androstane receptor and pregnane X receptor share xenobiotic and steroid ligands. *J Biol Chem* **275**: 15122–15127.

Rathore SS, Curtis JP, Wang Y, Bristow MR, Krumholz HM (2003). Association of serum digoxin concentration and outcomes in patients with heart failure [see comment]. *JAMA* **289**: 871–878.

Romiti N, Tramonti G, Chieli E (2002). Influence of different chemicals on MDR-1 P-glycoprotein expression and activity in the HK-2 proximal tubular cell line. *Toxicol Appl Pharmacol* **183**: 83–91.

Schinkel AH, Mayer U, Wagenaar E, Mol CA, Van Deemter L, Smit JJ *et al.* (1997). Normal viability and altered pharmacokinetics in mice lacking mdr1-type (drug-transporting) P-glycoproteins. *Proc Natl Acad Sci USA* **94**: 4028–4033.

Taipalensuu J, Tavelin S, Lazorova L, Svensson AC, Artursson P (2004). Exploring the quantitative relationship between the level of MDR1 transcript, protein and function using digoxin as a marker of MDR1-dependent drug efflux activity. *Eur J Pharmacol Sci* **21**: 69–75.

Takara K, Takagi K, Tsujimoto M, Ohnishi N, Yokoyama T (2003a). Digoxin upregulates multidrug resistance transporter (MDR1) mRNA and simultaneously downregulates steroid xenobiotic receptor mRNA [see comment]. *Biochem Biophys Res Commun* **306**: 116–120.

Takara K, Tsujimoto M, Kokufu M, Ohnishi N, Yokoyama T (2003b). Upregulation of MDR1 function and expression by cisplatin in LLC-PK1 cells. *Biol Pharmacol Bull* **26**: 205–209.

Takara K, Tsujimoto M, Ohnishi N, Yokoyama T (2002). Digoxin upregulates MDR1 in human colon carcinoma Caco-2 cells. *Biochem Biophys Res Commun* **292**: 190–194.

Thevenod F, Friedmann JM (1999). Cadmium-mediated oxidative stress in kidney proximal tubule cells induces degradation of Na+/K(+)-ATPase through proteasomal and endo-/lysosomal proteolytic pathways. *FASEB J* **13**: 1751–1761.

Tian R, Koyabu N, Morimoto S, Shoyama Y, Ohtani H, Sawada Y (2005). Functional induction and de-induction of P-glycoprotein by St John's wort and its ingredients in a human colon adenocarcinoma cell line. *Drug Metab Dispos* **33**: 547–554.

Vlaming ML, Mohrmann K, Wagenaar E, De Waart DR, Elferink RP, Lagas JS *et al.* (2006). Carcinogen and anticancer drug transport by Mrp2 *in vivo*: studies using Mrp2 (Abcc2) knockout mice. *J Pharmacol Exp Ther* **318**: 319–327.

Watkins RE, Wisely GB, Moore LB, Collins JL, Lambert MH, Williams SP *et al.* (2001). The human nuclear xenobiotic receptor PXR: structural determinants of directed promiscuity. *Science* **292**: 2329–2333.

Westphal K, Weinbrenner A, Zschiesche M, Franke G, Knoke M, Oertel R *et al.* (2000). Induction of P-glycoprotein by rifampin increases intestinal secretion of talinolol in human beings: a new type of drug/drug interaction. *Clin Pharmacol Ther* **68**: 345–355.

Zhou C, Tabb MM, Nelson EL, Grun F, Verma S, Sadatrafiei A *et al.* (2006). Mutual repression between steroid and xenobiotic receptor and NF-kappaB signaling pathways links xenobiotic metabolism and inflammation. *J Clin Invest* **116**: 2280–2289.